Polymer 51 (2010) 3116–3122

Contents lists available at ScienceDirect

Polymer

journal homepage: www.elsevier.com/locate/polymer

Monodisperse magnetic composite poly(glycidyl methacrylate)/$La_{0.75}Sr_{0.25}MnO_3$ microspheres by the dispersion polymerization

Daniel Horák [a,*], Miroslava Trchová [a], Milan J. Beneš [a], Miroslav Veverka [b], Emil Pollert [b]

[a] Institute of Macromolecular Chemistry AS CR, Heyrovského nám. 2, 162 06 Prague 6, Czech Republic
[b] Institute of Physics AS CR, Cukrovarnická 10, 162 53 Prague 6, Czech Republic

ARTICLE INFO

Article history:
Received 4 February 2010
Received in revised form
14 April 2010
Accepted 26 April 2010
Available online 20 May 2010

Keywords:
Magnetic
Dispersion polymerization
Glycidyl methacrylate

ABSTRACT

Monodisperse magnetic poly(glycidyl methacrylate) microspheres were prepared by dispersion polymerization of glycidyl methacrylate in cyclohexane in the presence of $La_{0.75}Sr_{0.25}MnO_3$ nanoparticles, surface of which was modified with penta(propylene glycol) methacrylate phosphate (PPGMAP). However, only agglomerates were formed by the dispersion polymerization in toluene. Sterical stabilizer was poly(styrene-*block*-hydrogenated butadiene-*block*-styrene) and initiators investigated were 2,2′-azobisisobutyronitrile (AIBN) and 4,4′-azobis(4-cyanovaleric acid) (ACVA). Effects of initiators and other reaction conditions on properties of the composite microspheres were evaluated. The phase composition of the magnetic polymer composite microspheres and the size of magnetic cores were determined by X-ray powder diffraction. The characterization was completed by magnetization measurements, atomic absorption spectroscopy, TEM, SEM and ATR FTIR spectroscopy.

1. Introduction

Encapsulation of magnetic particles in polymers prevents direct contact of magnetic substance with the environment and leads to their improved colloidal and chemical stability and reduced toxicity. At the same time, polymer surface can be modified allowing use of the particles in a wide variety of applications [1–3], such as water purification, separation and detection of cells, proteins and nucleic acids, immobilization of enzymes, diagnostics (immunoassays), therapeutics (drug targeting, hyperthermia) and catalysis. Various polymerization methods have been used to prepare magnetic polymer microspheres including miniemulsion [4], suspension [5], and dispersion [6,7] polymerization. Problems facing the preparation of such particles involve their coagulation, incomplete and nonuniform encapsulation of magnetic cores depending on the synthesis conditions. It is difficult to ensure that the polymerization takes place exclusively on the magnetic nanoparticle surface. Monodisperse micron-sized polymer particles can be produced by successive seeded emulsion polymerization [8] or activated swelling and polymerization (Ugelstad) method [9]. These processes are, however, complicated, time-consuming, and difficult to implement into a large scale due to a poor reproducibility. Moreover, encapsulation efficiencies are often insufficient. Emulsion or miniemulsion polymerizations are the most frequently used methods for the encapsulation of magnetic nanoparticles in polymers [10,11]. A small size of the resulting latex particles provides large surface area for functionalization, but the magnetic separation becomes more difficult. In emulsion polymerization, the main locus for particle nucleation is predominantly either in aqueous phase, which is called homogeneous nucleation, or in the monomer-swollen micelles called micellar nucleation, where large monomer droplets serve as reservoirs supplying monomer to the polymerizing particles [12]. Some micrometer-size polymer particles containing magnetic nanoparticles were synthesized also by the dispersion polymerization [7,13–15] which is attractive for large-scale preparation of such particles. Moreover, the dispersion polymerization offers an advantage of producing particles of a narrow size distribution in a single polymerization step. The polymerization consists of several stages including initiation in a homogeneous solution, precipitation of the polymer from the medium, formation of nuclei which then grow by polymerization or aggregation to form mature particles [16].

In our previous studies, dispersion polymerization of glycidyl methacrylate (GMA) in ethanol was developed [17], or magnetic poly(glycidyl methacrylate) (PGMA) particles were prepared in toluene/cyclohexane medium in the presence of surface-modified γ-Fe_2O_3 cores [18]. PGMA has an advantage of the presence of reactive oxirane groups which are easily modifiable to a variety of functional groups [19], such as aldehyde, aliphatic primary amino and diazotizable primary aromatic groups, suitable for prospective

* Corresponding author. Tel.: +420 296 809 260; fax: +420 296 809 410.
E-mail address: horak@imc.cas.cz (D. Horák).

0032-3861/$ – see front matter © 2010 Elsevier Ltd. All rights reserved.
doi:10.1016/j.polymer.2010.04.055

immobilization of enzymes and other proteins, nucleic acids or another required biomolecules. In order to improve incorporation of magnetic cores in PGMA microspheres, the cores were modified by heterobifunctional penta(propylene glycol) methacrylate phosphate (PPGMAP), a well-known polymerizable adhesion promoter [20,21]. In this report, an analogous procedure was used for the encapsulation of the lanthanum-manganese perovskite $La_{0.75}Sr_{0.25}MnO_3$ ferromagnetic cores of a mean size ~ 20 nm and Curie temperature of the transition to paramagnetic state at 63 °C [22]. This new hybrid material gives a promising chance of its application in the magnetic separation achieved by an applied static magnetic field switched on below the Curie temperature suitably adjusted at a selected value in the range 50–70 °C. In the next step, the magnetic field is switched off by moderate heating above the Curie temperature removing thus the remanency and transforming the cores into paramagnetic state. This promising technique is now under investigation and the results will be published elsewhere.

2. Experimental

2.1. Materials

Glycidyl methacrylate (GMA) from Fluka (Buchs, Switzerland) was vacuum-distilled before use. 2,2′-Azobisisobutyronitrile (AIBN; Fluka) was twice recrystallized from ethanol. 4,4′-Azobis(4-cyanovaleric acid) (ACVA) was from Aldrich (Milwaukee, WI, USA) and used as received. Kraton G 1650 (poly(styrene-*block*-hydrogenated butadiene-*block*-styrene); M_w = 74,000, M_n = 70,000; PSt/PBu = 29/71 w/w) was the stabilizer from Shell (Houston, TX, USA). Penta(propylene glycol) methacrylate phosphate (PPGMAP; Sipomer PAM 200) was obtained from Rhodia (France), toluene and cyclohexane from Lach–Ner (Neratovice, Czech Republic), all other chemicals were obtained from Aldrich. $La_{0.75}Sr_{0.25}MnO_3$ perovskite cores used for the encapsulation were prepared by the sol-gel method employing citric acid, ethylene glycol and La_2O_3, $SrCO_3$ and $MnCO_3$ as starting materials. The precursor was subjected to evaporation of water, drying, calcination and annealing for 3 h at 650–900 °C in air. In order to separate the individual crystallites and break connecting bridges formed during sintering, the product was subjected to mechanical treatment involving rolling and milling [23,24].

2.2. Modification of $La_{0.75}Sr_{0.25}MnO_3$ nanoparticles with PPGMAP

PPGMAP (0.7 g) was dissolved in ethanol (7 ml), $La_{0.75}Sr_{0.25}MnO_3$ particles (1 g) were added and the reaction proceeded at 23 °C for 20 h under stirring. Particles were six times washed with 30 ml of ethanol and dried.

2.3. Dispersion polymerization of GMA in the presence of PPGMAP-modified nanoparticles

In a 30-ml reactor, Kraton G 1650 (0.5 g) was dissolved in cyclohexane (10 g). Separately, dry PPGMAP-modified $La_{0.75}Sr_{0.25}MnO_3$ nanoparticles were dispersed in cyclohexane (4 g) under sonication for 5 min using a UP Ultrasonic processor (Hielscher Ultrasound Technology, Teltow, Germany) at 50% amplitude under cooling in cold water and AIBN (0.032 g) was dissolved in GMA (1.6 g). Both the dispersion and the solution were mixed together and added into the reactor under stirring (500, optionally 1000 rpm) and purged with nitrogen for 10 min. The polymerization was allowed to proceed at 70 °C for 8 h. After the polymerization, the microspheres were magnetically separated, seven times washed with cyclohexane (50 ml) to remove Kraton G 1650 and non-magnetic particles and finally dried under vacuum.

2.4. Characterization

Transmission electron microscopy (TEM; Tecnai Spirit G2; FEI, Brno, Czech Republic) and scanning electron microscopy (SEM; Jeol JSM 6400; Tokyo, Japan) were used for observation of the particles. Number-average diameter (D_n), weight-average diameter (D_w) and the uniformity (polydispersity index PDI = D_w/D_n) were calculated using Atlas software (Tescan Digital Microscopy Imaging, Brno, Czech Republic) by counting at least 500 individual particles (n_i) from the micrographs. The D_n and D_w can be expressed as follows:

$$D_n = \sum n_i \cdot D_i / \sum n_i$$

$$D_w = \sum n_i \cdot D_i^4 / \sum n_i \cdot D_i^3$$

Attenuated total reflection (ATR) FTIR spectroscopy. Functionalization of the surface of the magnetic cores with PPGMAP was investigated using a Thermo Nicolet Nexus 870 FTIR Spectrometer (Madison, WI, USA) in an H_2O-purged environment with the liquid nitrogen cooled mercury cadmium telluride (MCT) detector in the range from 650 to 4000 cm^{-1}. The Golden Gate™ Heated Diamond ATR Top-Plate (MKII Golden Gate single reflection ATR system; Specac Ltd., Orpington, Great Britain) was used for the measurements of spectra of the powdered samples by ATR spectroscopic technique. Typical parameters were: 256 scans, resolution 4 cm^{-1}, Happ-Genzel apodization, KBr beamsplitter.

Mn content was determined by a Perkin–Elmer 3110 (Norwalk, CT, USA) atomic absorption spectrometer (AAS) using air-acetylene flame. Analyzed solution was obtained by mineralization of a sample with concentrated perchloric (1 ml) and nitric acid (0.3 ml). The content of $La_{0.75}Sr_{0.25}MnO_3$ in PGMA microspheres was calculated from Mn content.

The phase composition of the magnetic $La_{0.75}Sr_{0.25}MnO_3$ nanoparticles/polymer composite microspheres and the crystallite size of magnetic nanoparticles were determined by X-ray powder diffraction using a Bruker D8 diffractometer (CuK_α radiation, Sol-X energy dispersive detector). X-ray diffraction patterns were analyzed by the Rietveld method using the FULLPROF program (Version 2.20-Sep2002-LLB JRC). The crystallite size delimits the XRD coherence length and thus contributes to the peak width. The Thompson-Cox-Hastings pseudo-Voigt profile was used to resolve instrumental, strain and size contributions to peak broadening. Instrumental resolution was determined by measuring strain-free tungsten powder with crystallite size 9.41 μm. Magnetic properties were measured with a SQUID magnetometer MPMS5 (Quantum Design, San Diego, USA) at 295 K and the fields up to 1.5 kA m^{-1}.

3. Results and discussion

3.1. Surface modification of $La_{0.75}Sr_{0.25}MnO_3$ with PPGMAP

A condition of crucial importance for a successful encapsulation of $La_{0.75}Sr_{0.25}MnO_3$ nanoparticles by a hydrophobic polymer such as PGMA is their compatibilization with the GMA monomer. Therefore PPGMAP was selected as a compatibilizing agent to provide encapsulation of $La_{0.75}Sr_{0.25}MnO_3$ nanoparticles into the PGMA microspheres. It has a phosphate group anchoring to the nanoparticle surface and also contains a polymerizable olefinic group, providing a covalent attachment of PGMA chains to $La_{0.75}Sr_{0.25}MnO_3$ surface during the subsequent dispersion polymerization. If $La_{0.75}Sr_{0.25}MnO_3$ nanoparticles without PPGMAP

were used in the dispersion polymerization of GMA, the nanoparticles were not encapsulated. PPGMAP thus contributes to the dispersing of the magnetic nanoparticles inside the PGMA microspheres.

Fig. 1 shows the typical TEM micrograph of PPGMAP-coated $La_{0.75}Sr_{0.25}MnO_3$ nanoparticles. The *ca.* 20 nm originally well-separated particles by the mechanical treatment [23,24] have a tendency to be connected together in *ca.* 100 nm aggregates.

The interaction between the PPGMAP and the surface of the $La_{0.75}Sr_{0.25}MnO_3$ nanoparticles was studied by ATR FTIR spectroscopy. The spectra confirmed that the surface modification of $La_{0.75}Sr_{0.25}MnO_3$ with PPGMAP was successful, which is in an agreement with our previous results [25]. The shape of the differential spectrum is very close to the spectrum of pure PPGMAP (Fig. 2) and shows markedly a shielding effect of the coating. The shift of the maximum of the band of P–O and C–O stretching vibrations from the 1000 cm^{-1} observed in the spectrum of pure PPGMAP to the 1100 cm^{-1} in the differential spectrum is probably connected with the different contacts of the uncoated and coated nanoparticles with the ATR crystal during the measurement and with the interaction between the PPGMAP and the nanoparticle surface via P–OH groups. No shielding effect in the region of C=O and C=C vibrations has been detected which supports the fact, that only the interaction of phosphate groups comes into the consideration. The carbon content in the modified $La_{0.75}Sr_{0.25}MnO_3$ nanoparticles was 4.15 wt.% which corresponded to 8.2 wt.% PPGMAP.

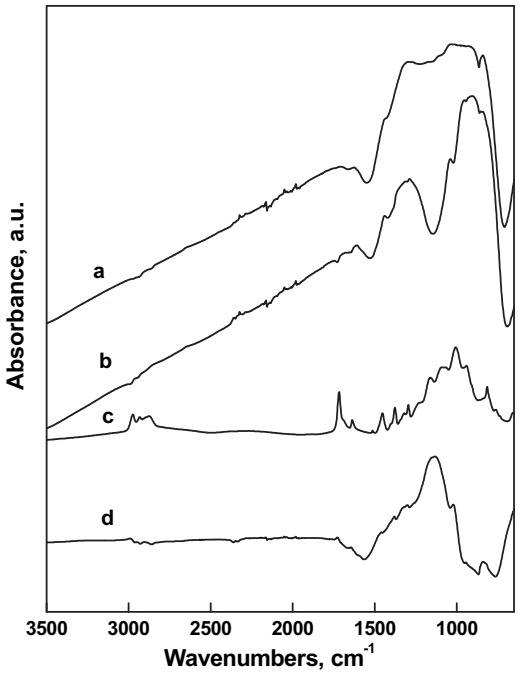

Fig. 2. ATR FTIR spectra of $La_{0.75}Sr_{0.25}MnO_3$ before and after the surface modification; (a) spectrum of $La_{0.75}Sr_{0.25}MnO_3$ before modification, (b) after coating with PPGMAP, (c) spectrum of neat PPGMAP, and (d) differential spectrum (spectrum of unmodified − spectrum of modified nanoparticles). The spectra are shifted for clarity.

3.2. Encapsulation of PPGMAP-modified $La_{0.75}Sr_{0.25}MnO_3$ nanoparticles by the dispersion polymerization of GMA

The PPGMAP-modified $La_{0.75}Sr_{0.25}MnO_3$ nanoparticles were first dispersed in toluene and GMA was polymerized in their presence. However, the Kraton G 1650-stabilized and AIBN-initiated dispersion polymerization of GMA in toluene in the presence of PPGMAP-coated $La_{0.75}Sr_{0.25}MnO_3$ nanoparticles yielded agglomerates on the stirrer; irregular submicrometer particles were obtained only partly (Fig. 3). Agglomeration was probably induced by a partial solubility of PGMA in toluene which is not tolerable in the dispersion polymerization. Therefore, in the following experiments the toluene polymerization medium was replaced by cyclohexane, in which PGMA is completely insoluble. At the same time, the concentrations of GMA (11 wt.%) and Kraton G 1650 stabilizer (3.6 wt.%) in cyclohexane were fixed and the polymerization temperature was kept at 70 °C. The presence of the Kraton G 1650 steric stabilizer is required to suppress particle aggregation. The polymer was then obtained in a form of the free-flowing powder constituted of submicrometer microspheres in an almost quantitative yield. The effects of some variables, such as the PPGMAP-modified $La_{0.75}Sr_{0.25}MnO_3$/GMA ratio and the initiator

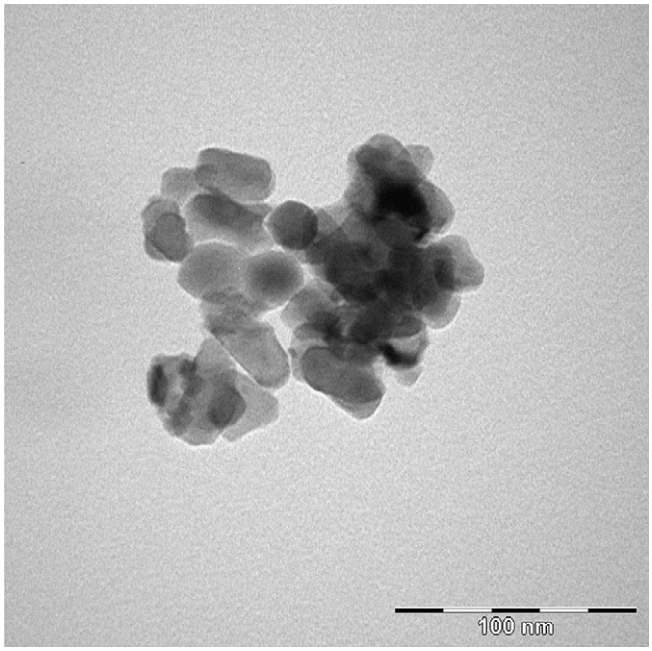

Fig. 1. TEM micrograph of PPGMAP-coated $La_{0.75}Sr_{0.25}MnO_3$ nanoparticles.

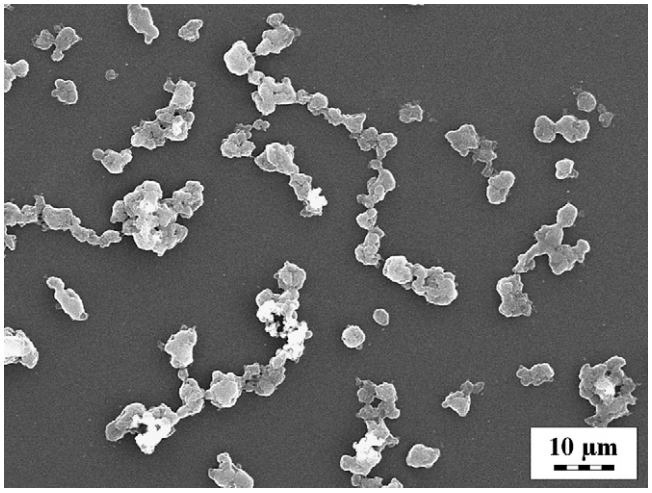

Fig. 3. SEM micrograph of magnetic PGMA microspheres obtained by the AIBN-initiated dispersion polymerization in toluene. PPGMAP-modified $La_{0.75}Sr_{0.25}MnO_3$/GMA ratio = 0.125 (w/w); 2 wt.% AIBN initiator relative to monomers.

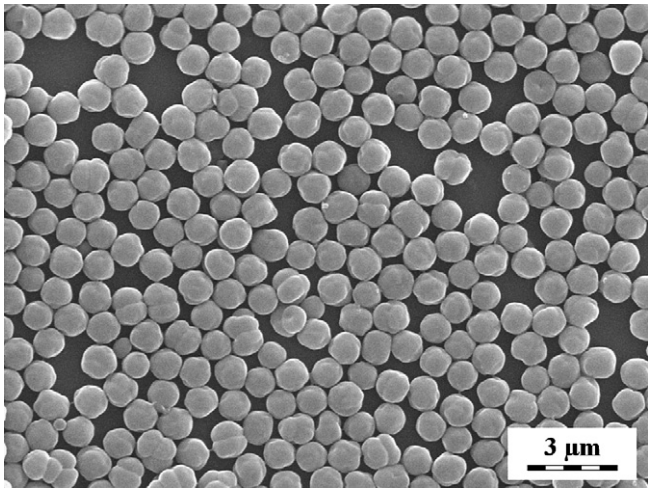

Fig. 4. SEM micrograph of non-magnetic PGMA microspheres obtained by the AIBN-initiated dispersion polymerization in cyclohexane; 2 wt.% AIBN initiator relative to monomers.

and its concentration on the properties of the PGMA microspheres were investigated.

3.3. The effect of PPGMAP-modified $La_{0.75}Sr_{0.25}MnO_3$/GMA ratio on the dispersion polymerization

First, Kraton G 1650-stabilized and AIBN-initiated dispersion polymerization of GMA in cyclohexane was investigated in the absence of $La_{0.75}Sr_{0.25}MnO_3$ particles. As a result, monodisperse *ca.* 1 µm non-magnetic PGMA microspheres were formed (Fig. 4). The dispersion polymerization always starts from a homogeneous solution of a monomer and all other reactants (including polymeric stabilizer and initiator) in the reaction medium. As oligomer chains grow in size and eventually reach a molecular weight exceeding a critical value, they precipitate from solution and aggregate forming colloidally unstable precursor particles (nuclei). These particles coalesce and adsorb stabilizers from the reaction medium onto their surface until they become colloidally stable. At this point, the total number of particles in the system is fixed, and the nucleation stage ceases. The subsequent polymerization, called the particle growth stage, occurs either inside the monomer-swollen nuclei or in the reaction medium depending on the polymer–solvent interactions. However, the newly formed polymer molecules do not form additional nuclei but they are captured by existing particles [26].

Table 1
Effect of the PPGMAP-modified $La_{0.75}Sr_{0.25}MnO_3$/GMA ratio on the PGMA microsphere size D_n at (△) 2 wt.% and (□) 5 wt.% AIBN in monomers.

PPGMAP-$La_{0.75}Sr_{0.25}MnO_3$/GMA (w/w)	D_n (µm)	
	2 wt.% AIBN	5 wt.% AIBN
0	0.98	0.82
0.06	0.68	–
0.12	0.46	0.63
0.19	0.73	0.47
0.25	–	0.62
0.31	0.59	0.57

The nucleation stage in the dispersion polymerization is very sensitive to variations in reaction components or conditions. It has been found that the incorporation of functional monomers [27] or cross-linking agents [28] in the dispersion polymerization mixture is much more difficult than it is in other heterogeneous polymerizations such as emulsion polymerization. Also the addition of PPGMAP-modified $La_{0.75}Sr_{0.25}MnO_3$ nanoparticles in the polymerization system changed properties of the product. Double bond of the methacrylate end unit of PPGMAP copolymerizes with GMA; as a result, PGMA is thus grafted on the $La_{0.75}Sr_{0.25}MnO_3$ cores. It was interesting that the encapsulation of a small amount of PPGMAP-coated $La_{0.75}Sr_{0.25}MnO_3$ nanoparticles (PPGMAP-modified $La_{0.75}Sr_{0.25}MnO_3$/GMA ratio ≤ 0.06) in the feed containing 2 or 5 wt.% of AIBN relative to monomers resulted in a decrease of the PGMA microsphere size of a narrow size distribution (Table 1). This can be explained by an improved stabilization of the PPGMAP-coated $La_{0.75}Sr_{0.25}MnO_3$. The particle size, however, remained almost unchanged with a further increase of PPGMAP-modified $La_{0.75}Sr_{0.25}MnO_3$/GMA ratio exceeding 0.06 (Table 1). The presence of manganese perovskite phase inside the PGMA microspheres was evidenced with TEM micrographs of ultrathin cross-sections of the microspheres before purification by magnetic separation (Fig. 5). The encapsulated $La_{0.75}Sr_{0.25}MnO_3$ nanoparticles were evident as domains of high contrast distributed within the low contrast PGMA sphere (Fig. 5). This demonstrated that the presence of PPGMAP was required for the effective encapsulation in the present system. TEM showed that the number of $La_{0.75}Sr_{0.25}MnO_3$ nanoparticles in each microsphere varied (Fig. 5). Like in many other reports on composite particles [29,30], formation of “empty” particles (those

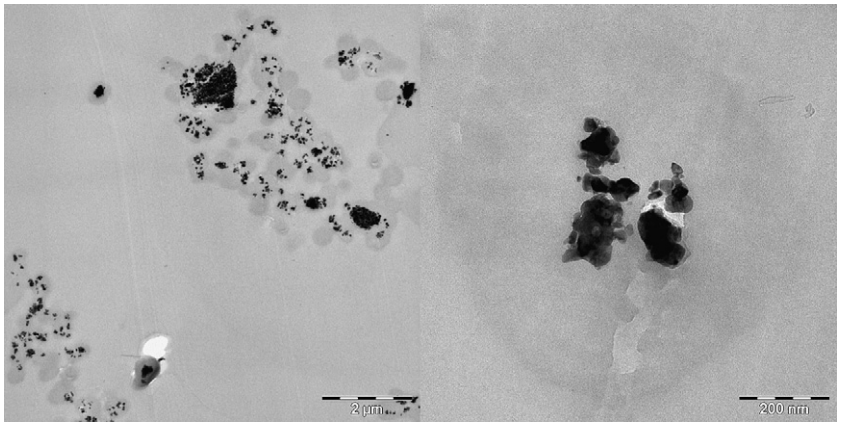

Fig. 5. Representative TEM micrographs of ultrathin cross-sections of magnetic PGMA microspheres embedded in London Resin White; black – magnetic cores, grey – PGMA. The microspheres were prepared at the PPGMAP-modified $La_{0.75}Sr_{0.25}MnO_3$/GMA ratio 0.31 (w/w); 5 wt.% AIBN relative to monomers. TEM images were taken before purification by magnetic separation.

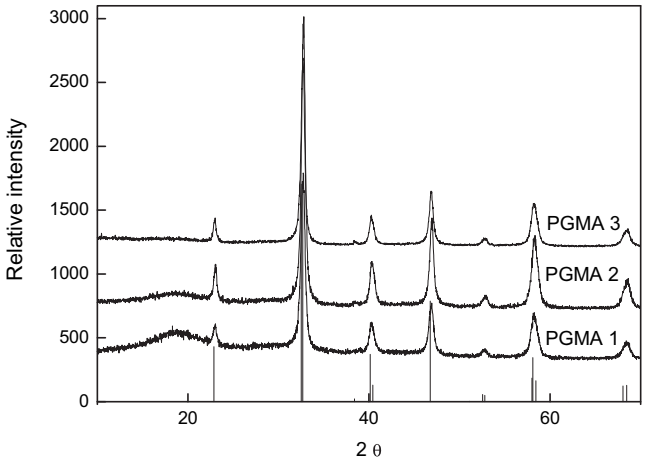

Fig. 6. X-ray powder analysis of magnetic PGMA microspheres; solid lines – manganese perovskite phase.

encapsulating no $La_{0.75}Sr_{0.25}MnO_3$) was difficult to avoid due to the nucleation of new polymer particles (Fig. 5). "Empty" (non-magnetic) particles are, however, easy to remove by careful purification using magnetic separation. Thus, it can be concluded, that according to TEM of cross-sections of PGMA microspheres, PPGMAP-coated $La_{0.75}Sr_{0.25}MnO_3$ particles were located in the interior. The encapsulation was additionally confirmed by X-ray powder analysis (Fig. 6). Amorphous polymer shell was only slightly detectable in the range of the diffraction angles ~ 15–22 ° θ for the PGMA 1 and PGMA 2 microspheres. Mean size of the $La_{0.75}Sr_{0.25}MnO_3$ cores d_{XRD} = 20 nm was determined from the broadening of the diffraction peaks, delimited by the coherence length. Magnetization curves confirmed an expected gradual increase of the magnetization with an increasing content of the lanthanum–manganese perovskite phase in the PGMA microspheres (Fig. 7). Using the magnetization value $M_{750\ kA/m}$ = 24 A m^2 kg^{-1} of the pure synthesized manganese perovskite (size 20 nm), the contents of $La_{0.75}Sr_{0.25}MnO_3$ magnetic phase in the PGMA 1–3 microspheres were evaluated (Table 2). Simultaneously, an independent analytical method, namely AAS, confirmed an expected increase of the content of $La_{0.75}Sr_{0.25}MnO_3$ in the microspheres from 13 to 47.6 wt.% with an increasing PPGMAP-modified $La_{0.75}Sr_{0.25}MnO_3$ content in the feed from 15.7 to 23.8 wt.%

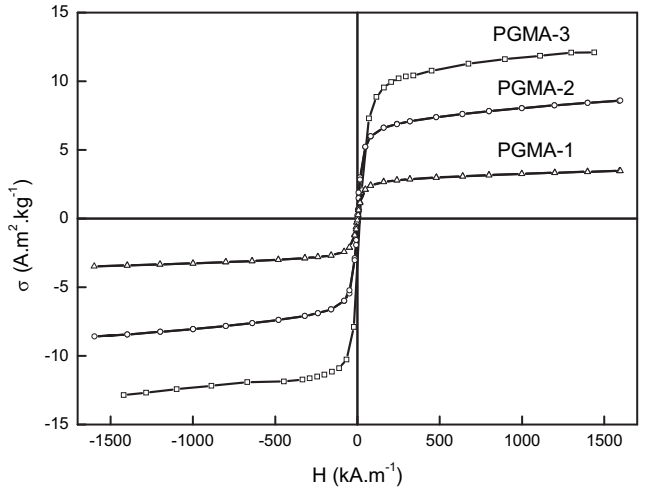

Fig. 7. Magnetization curves of the magnetic PGMA microspheres.

Table 2
Content of $La_{0.75}Sr_{0.25}MnO_3$ (wt.%) in the polymerization feed and in magnetic PGMA microspheres.

Sample	In the feed	In the microspheres	
		Determined by AAS	Calculated from the magnetization data
PGMA 1	15.7	13.0	13.0
PGMA 2	20	32.7	32.5
PGMA 3	23.8	47.6	47.2

Dispersion polymerization in cyclohexane was initiated by 5 wt.% AIBN relative to monomers.

(Table 2), in agreement with the data determined from the magnetization measurements. A seeming discrepancy between contents of $La_{0.75}Sr_{0.25}MnO_3$ in the feeds and substantially higher contents in the microspheres (samples PGMA 2 and PGMA 3 in Table 2) was a consequence of the formation of non-magnetic microspheres which were removed during the washing procedures.

3.4. The effect of AIBN and ACVA initiators

Oil-soluble azo initiators, AIBN or ACVA, were used to start the dispersion radical polymerization of GMA in the presence of

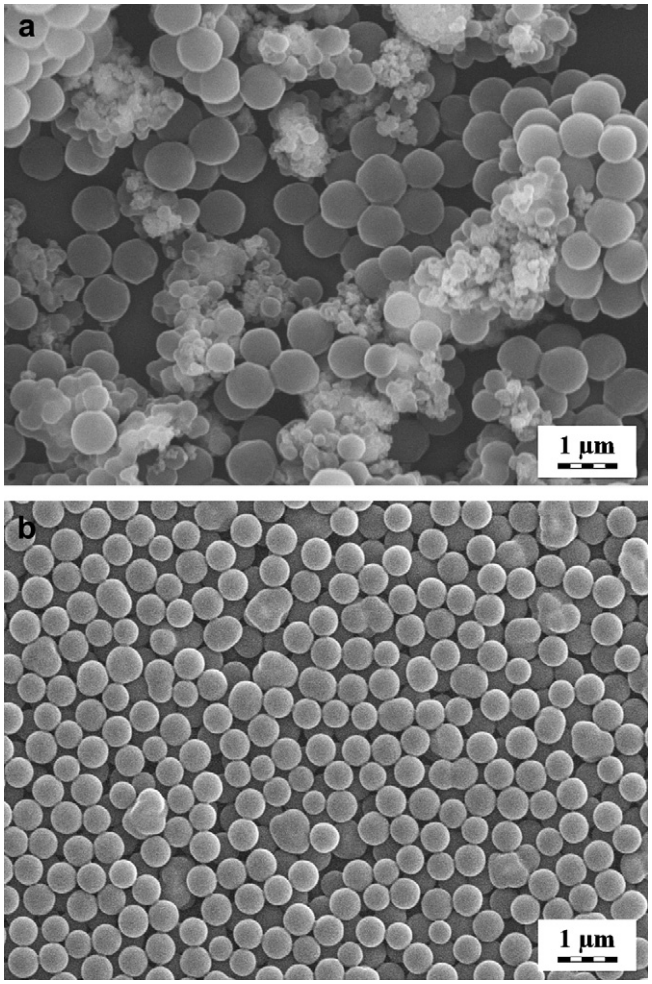

Fig. 8. SEM micrographs of magnetic PGMA microspheres obtained by the AIBN-initiated dispersion polymerization in cyclohexane. PPGMAP-modified $La_{0.75}Sr_{0.25}MnO_3$/GMA ratio = (a) 0.31 and (b) 0.19 (w/w); (a) 2 wt.% and (b) 5 wt.% AIBN initiator relative to monomers.

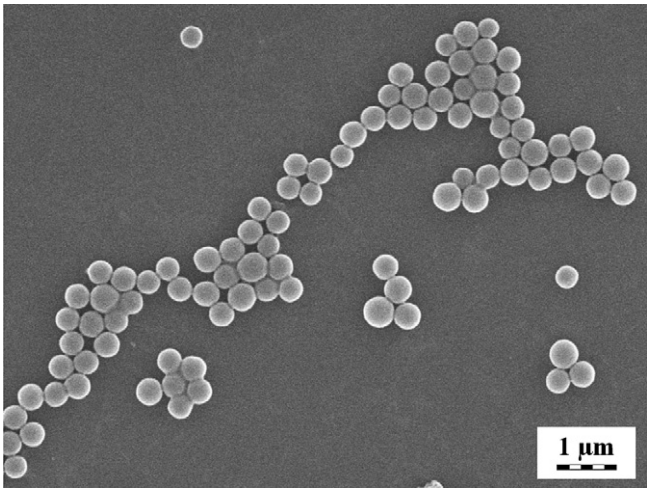

Fig. 9. SEM micrograph of magnetic PGMA microspheres obtained by the ACVA-initiated dispersion polymerization in cyclohexane. PPGMAP-modified $La_{0.75}Sr_{0.25}MnO_3$/GMA ratio = 0.31 (w/w) and 0.85 wt.% ACVA initiator relative to monomers.

PPGMAP-modified $La_{0.75}Sr_{0.25}MnO_3$ nanoparticles. They differ in a decomposition rate in toluene at the reaction temperature 70 °C with a half-time of decomposition 289 min for the first and 252 min for the second initiator [31]. A comparative study of the effect of two AIBN concentrations (2 and 5 wt.% in the monomers) on the properties of the microspheres showed no influence on their size which was found in the range of 0.5–1 μm (Table 1). In the system with a high PPGMAP-modified $La_{0.75}Sr_{0.25}MnO_3$/GMA ratio (0.31 w/w), initiated by 2 wt.% of AIBN, two families of the microspheres were formed, i.e., a large one, consisting of *ca.* 0.7 μm particles, and a small one, containing *ca.* 0.2 μm particles in diameter (Fig. 8a). Evidently, the broad size distribution obtained at a high PPGMAP-modified $La_{0.75}Sr_{0.25}MnO_3$/GMA ratio can be attributed to the prolonged nucleation period. Two origins of loss of monodispersity can be considered. One occurs when there is an excess of stabilizer available, which can stabilize a second crop of smaller polymer particles. The other possibility is that the number of molecules of the stabilizer is too low to stabilize the growing polymer surface, thus leading to a certain degree of coalescence.

However, at higher AIBN concentrations (5 wt.%) monodisperse magnetic PGMA microspheres were obtained (Fig. 8b) because nucleation was fast enough and formation of the second crop of small particles was suppressed. Thus, the particle number and the particle size distribution were determined during the nucleation stage and no secondary particles or coagulum were formed during the particle growth stage [32,33].

Microspheres obtained by the ACVA-initiated dispersion polymerizations were smaller in size, typically < 0.5 μm, than those prepared from the AIBN-initiated systems. This can be ascribed to the precipitation of shorter oligomeric chains in the ACVA than in the AIBN initiation systems due to a relatively faster decomposition of ACVA. It results in the formation of higher number of nuclei which are in turn smaller in size. The fast decomposition rate of ACVA associated with a short nucleation period was also the reason for the production of monodisperse magnetic PGMA microspheres at a low ACVA concentration 0.85 wt.% relative to monomers (Fig. 9). The observed variation of the PGMA microsphere size with the ACVA initiator concentration (Table 3) can be attributed to a competition of two polymerization mechanisms, coagulation and homogeneous nucleation [34]. First, a coagulation mechanism is decisive. An increasing concentration of the initiator leads to an instantaneous increase in the concentration of the growing oligomeric radicals and their association. As a result, a limited amount of relatively large particles is formed. When a critical ACVA concentration is reached, i.e. about 1 wt.%, the coagulation nucleation mechanism is gradually replaced by a homogeneous nucleation proposed by Fitch and Tsai [34]. It leads to a formation of a large number of primary particles of a limited size. At the same time, with an increasing concentration of ACVA the microspheres had an increasing tendency to aggregate (PDI > 1.2). Nevertheless, a complete elucidation of the effect of the ACVA initiator concentration on the properties of the microspheres requires a further investigation which is in progress.

Table 3
Variation of the magnetic PGMA microsphere size D_n and polydispersity index *PDI* with the concentration of ACVA initiator *c* (relative to monomers). PPGMAP-modified $La_{0.75}Sr_{0.25}MnO_3$/GMA ratio = 0.31 (w/w).

c (wt.%)	0.42	0.85	1.7	2.6	4.25
D_n (μm)	0.27	0.417	0.385	0.232	0.311
PDI	1.215	1.023	1.075	1.238	1.182

4. Conclusions

Conditions of the dispersion polymerization of GMA in the presence of the perovskite $La_{0.75}Sr_{0.25}MnO_3$ magnetic cores were optimized. The surface modification of the manganese perovskite nanoparticles by PPGMAP improved their compatibility with GMA and facilitated thus their incorporation into the PGMA microspheres. The effect of PPGMAP-modified $La_{0.75}Sr_{0.25}MnO_3$/GMA ratio and of the initiator type and concentration on the properties of the resulting microspheres was investigated. With the concentration of the AIBN initiator at 5 wt.% (relative to monomers) and with the gradual increase of $La_{0.75}Sr_{0.25}MnO_3$ amount in the feed, the content of the $La_{0.75}Sr_{0.25}MnO_3$ in the microspheres increased; this was in agreement with the increase of the magnetization. At the same time, this high AIBN concentration yielded monodispersity of the magnetic PGMA microspheres. In contrast, only a low concentration of ACVA initiator (0.85 wt.%) was required to obtain a narrow particle size distribution. The achieved monodispersity was obviously induced by a short nucleation period, after which neither new nucleation nor coagulation took place.

The newly developed microspheres are primarily suitable for the magnetic separation of biomolecules after their immobilization on properly modified reactive oxirane groups. Ring opening of oxirane groups makes easy introduction of amino or thiol groups, which are, e.g., suitable for covalent attachment of enzymes and affinity ligands. In addition, it may be possible to actively drive and direct the movement of such particles for application in biomolecule delivery and microfluidics.

Acknowledgement

Financial support of AS CR, projects KAN200200651 and KAN201110651, Grant Agency of the Czech Republic, grant 203/09/0857, and Ministry of Education, Youth and Sports, grant 2B06053, is gratefully acknowledged.

References

[1] Ugelstad J, Berge A, Ellingsen T, Schmid R, Nilsen T-N, Mork PC, et al. Prog Polym Sci 1992;17:87–161.
[2] Horák D, Babič M, Macková H, Beneš MJ. J Sep Sci 2007;30:1751–72.
[3] Lu AH, Salabas EL, Schüth F. Angew Chem Int Ed 2007;46:1222–44.
[4] Faridi-Majidi R, Sharifi-Sanjani N. J Magn Magn Mater 2007;311:55–8.
[5] Ma Z, Guan Y, Liu X, Liu H. Polym Adv Technol 2005;16:554–8.
[6] Zeng HM, Lai QY, Liu XQ, Wen D, Ji XY. J Appl Polym Sci 2007;106:3474–80.
[7] Horák D, Boháček J, Šubrt M. J Polym Sci Polym Chem Ed 2000;38:1161–71.
[8] Vanderhoff WJ. Chem Eng Sci 1993;48:203–17.

[9] Ugelstad J, Ellingsen T, Berge A, Helgee B. Magnetic polymer particles and process for the preparation thereof. Eur. Patent WO 83/03920; 1983.
[10] Yanase N, Noguchi H, Asakura H, Suzuta T. J Appl Polym Sci 1993;50:765–76.
[11] Ramírez LP, Landfester K. Macromol Chem Phys 2003;204:22–31.
[12] Chern CS. Prog Polym Sci 2006;31:443–86.
[13] Wang P-C, Lee C-F, Young T-H, Lin D-T, Chiu W-Y. J Polym Sci A Polym Chem 2005;43:1342–56.
[14] Wang P-C, Chiu W-Y, Lee C-F, Young T-H. J Polym Sci A Polym Chem 2004;42:5695–705.
[15] Horák D, Benedyk N. J Polym Sci Polym Chem Ed 2004;42:5827–37.
[16] Ober CK. Makromol Chem Macromol Symp 1990;35/36:87–104.
[17] Horák D, Shapoval P. J Polym Sci Part A Polym Chem Ed 2000;38:3855–63.
[18] Tocchio A, Horák D, Babič M, Trchová M, Veverka M, Beneš MJ, et al. J Polym Sci Polym Chem Ed 2009;47:4982–94.
[19] May AC, editor. Epoxy resins: Chemistry and technology. New York: Dekker; 1988.
[20] Gonzalez I, Mestach D, Leiza JR, Asua JM. Prog Org Coat 2008;61:38–44.
[21] Yang HS, Adam H, Kiplinger J. JCT Coatingstech 2005;2:44–52.
[22] Kaman O, Pollert E, Veverka P, Veverka M, Hadová E, Knížek K, et al. Nanotechnology 2009;20:275610–7.
[23] Vasseur S, Duguet E, Portier J, Goglio G, Mornet S, Hadová E, et al. J Magn Magn Mater 2006;302:315.
[24] Pollert E, Knížek K, Maryško M, Kašpar P, Vasseur S, Duguet E. J Magn Magn Mater 2007;316:122–5.
[25] Horák D, Pollert E, Trchová M, Kovářová J. Eur Polym J 2009;45:1009–16.
[26] Kawaguchi S, Ito K. Adv Polym Sci 2005;175:299–328.
[27] Yang W, Yang D, Hu J, Wang C, Fu S. J Polym Sci Part A Polym Chem 2001;39:555–61.
[28] Song JS, Winnik MA. Macromolecules 2005;38:8300–7.
[29] Joumaa N, Tossay P, Lansalot M, Eliassari A. J Polym Sci Part A Polym Chem 2008;46:327–40.
[30] Tiarks F, Landfester K, Antonietti M. Macromol Chem Phys 2005;202:51–60.
[31] Brandrup J, Immergut EH, Grulke AE. Polymer Handbook. New York: J. Wiley; 1999.
[32] LaMer VK, Dinegar RH. J Am Chem Soc 1950;72:4847–54.
[33] Sáenz JM, Asua JM. J Polym Sci Polym Chem Ed 1995;33:1511–21.
[34] Fitch RM. Polymer colloids: A comprehensive introduction. San Diego: Academia Press; 1997.